Available online at www.sciencedirect.com
ScienceDirect
Ceramics International 36 (2010) 1041–1045
CERAMICS INTERNATIONAL
www.elsevier.com/locate/ceramint

Phase evolution, dielectric and impedance spectroscopic study of $SrNb_2O_6$ columbite phase

M. Pastor [a], S. Goenka [b], S. Maiti [a], K. Biswas [a,*], I. Manna [a]

[a] Department of Metallurgical & Materials Engineering, Indian Institute of Technology, Kharagpur 721302, India
[b] Department of Metallurgy, Punjab Engineering College, Chandigarh 160012, India

Received 11 June 2009; received in revised form 9 July 2009; accepted 16 November 2009
Available online 4 January 2010

Abstract

Strontium niobate $SrNb_2O_6$ has been synthesized by columbite solid-state reaction method and characterized by X-ray diffraction (XRD), scanning electron microscope (SEM) and temperature as well as frequency dependence of dielectric and impedance study. XRD analysis indicates single phase formation of the compound with ~180 nm crystallite size. Study of SEM micrographs pointed out that prepared material has good sinterability and enough density with homogeneous grain distribution. It was found that the magnitude of relative dielectric constant (ε_r) was relatively high with low dielectric loss compared with reported columbite compounds. Impedance spectroscopy was used to characterize the electrical behavior of the compound. AC impedance spectrum results indicate that the relaxation mechanism of the material is temperature dependent and has bulk and grain boundary contribution in different temperature ranges.

Keywords: C. Dielectric properties; Electronic materials; Impedance spectroscopy; X-ray diffraction

1. Introduction

Divalent columbite niobate ceramics with general formula ANb_2O_6 (A = divalent cations) have very interesting characteristics as excellent dielectric property, quality factor and temperature coefficient of resonant frequency [1–3]. Therefore, they have been characterized for the application point of view in microwave resonators. Many attempts have been done to get single columbite phase in these materials but it is found very difficult because of corundum like phase, and requires prolonged heating [4].

Most of the ANb_2O_6 compounds also exhibit polymorphism; however, each can exist as an isomorphous orthorhombic phase with the columbite structure, except for the Sr, Ba and Pb analogues which crystallize in a different orthorhombic structures [5]. These niobates also have very important role in the synthesis of perovskite with general formula $A'(B'_{1/3}B''_{2/3})O_3$ type materials (where $A' = Pb^{2+}$, Ba^{2+} or Sr^{2+}; $B' = Mg^{2+}$, Zn^{2+}, Ni^{2+}, Co^{2+}, or Mn^{2+} and $B'' = Nb^{5+}$) [6–14]. In the present investigation, efforts were made to prepare $SrNb_2O_6$ ceramics using simple solid-state reaction route. Earlier reports also suggested that it is very difficult to prepare single columbite phase by solid-state reaction route [15].

There are no reports on impedance study of $SrNb_2O_6$ sintered compound. Therefore, present work is mainly aimed to study (a) attempt to get single columbite phase $SrNb_2O_6$ by solid-state reaction route, (b) dielectric study and (c) impedance study of $SrNb_2O_6$ and correlation with structural parameters.

2. Experimental

Columbite structure was formed by pre-reacting Nb_2O_5 (99.9% Loba Chemie Pvt. Ltd., India) with $SrCO_3$ (99.9% pure, M/s B.D.H. Chemicals, UK) followed by calcination at 1100 °C for 8 h. Calcined powder was then characterized by X-ray diffraction technique (XRD) (Philips (PW1710) X-ray diffractometer (Co Kα radiation, λ = 0.17890 nm) to ensure the formation of columbite structure.

The fine and homogeneous powder of the above compound with PVA binder was pressed into cylindrical pellets of 10 mm diameter and 1–2 mm thickness under a uniaxial pressure of 300 MPa using a hydraulic press. The compacted pellets were

* Corresponding author. Tel.: +91 3222 283244; fax: +91 3222 282280.
E-mail address: k_biswas@metal.iitkgp.ernet.in (K. Biswas).

0272-8842/$36.00
doi:10.1016/j.ceramint.2009.12.013

first fired at 500 °C to remove the binder and then sintered at 1275 °C for 12 h to get highly dense sample (∼95%).

The X-ray powder diffraction pattern of calcined powder was taken at room temperature. The microstructure and grain size distribution of the sintered pellets were studied by scanning electron micrograph using scanning electron microscope (JEOL JSM-5800, Japan) at 20 kV. The dielectric and impedance spectroscopic data were recorded on polished sintered pellets as a function of temperature from room temperature to 350 °C using impedance analyzer (HIOKI 3532 LCR Hi TESTER, Japan) with perturbation voltage was of 1.2 V.

3. Results and discussion

The X-ray diffractogram (XRD) (Fig. 1) of calcined powder comprising of sharp diffraction peaks of varying intensity that is different from those of precursor materials confirms the formation of $SrNb_2O_6$ phase. The peaks have been successfully indexed using standard computer software (POWDMULT) [16]. A preliminary structural analysis indicates that the system under investigation has orthorhombic (columbite) structure. The lattice parameters as evaluated using the software were refined by the least square refinement method. The calculated values are in well agreement with the structural data as reported in JCPDS file [28-1243] and found to be $a = 11.00$, $b = 7.714$ and $c = 5.603$ Å. Density has been calculated by Archimedes principle and found to be ∼96%. Scanning electron micrographs of the sintered powders (Fig. 2) reveal that sintering produces fairly dense and homogenous product with very little porosity. Enhanced sintering capabilities can be attributed to the micron-sized dimensions of the calcined powders. The grains of the materials after sintering have typical dimension in the range ∼1.8–3.0 μm.

Fig. 3(a) reveals the temperature dependence relative dielectric constant (ε_r) at different (1, 5, 10, 50 and 100 kHz.) frequencies. The variation of tangent loss (tan δ) with temperature is also shown in Fig. 3(b). The ε_r increases with rise in temperature up to its maximum value ($\varepsilon_{r\,(max)}$) at the Curie temperature (T_c), and then decreases with further increase in temperature. The value of ε_r at room temperature, $\varepsilon_{r\,(max)}$ and T_c are given in Table 1 at studied frequencies. The room

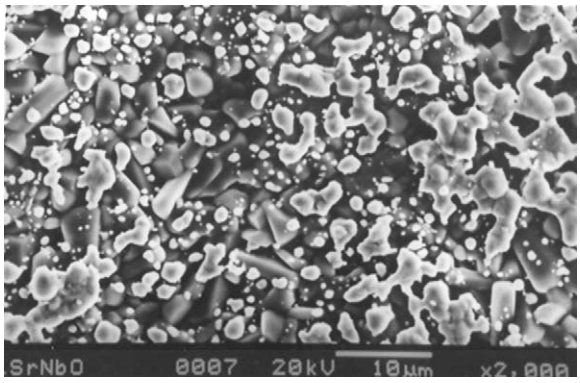

Fig. 2. SEM microstructure of $SrNb_2O_6$ at room temperature.

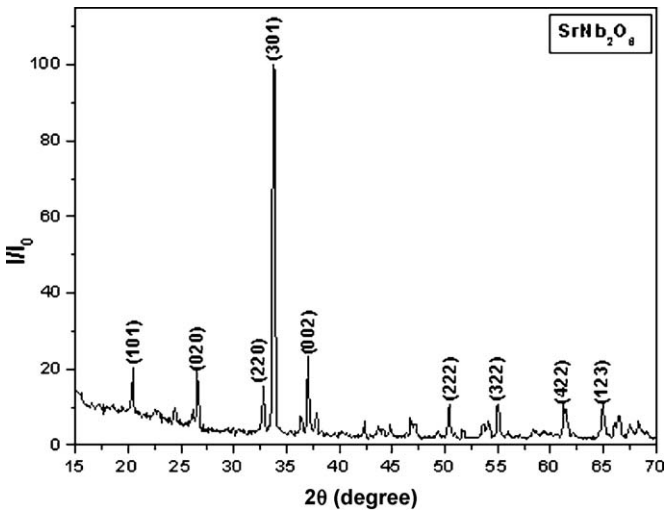

Fig. 1. X-ray diffraction profiles of $SrNb_2O_6$ calcined powder at room temperature.

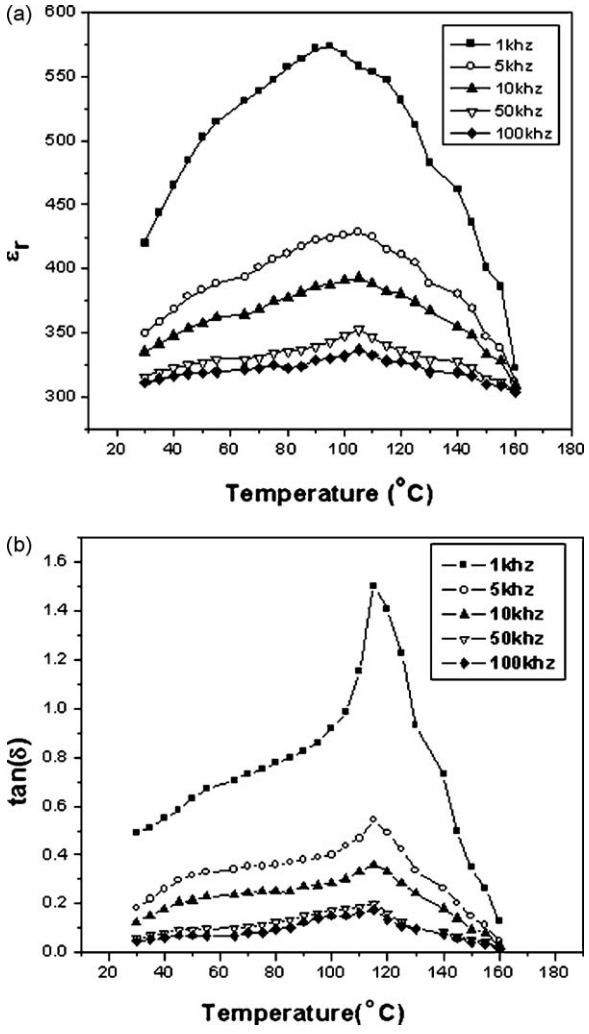

Fig. 3. (a) Variation of relative permittivity (ε_r) of $SrNb_2O_6$ with temperature at different frequencies. (b) Variation of tan δ of $SrNb_2O_6$ with temperature at different frequencies.

Table 1
Dielectric parameters of $SrNb_2O_6$ at different frequencies.

Frequency (kHz)	T_c (°C)	$\varepsilon_{r\ (max)}$	ε_r at room temperature
1	95	573	420
5	105	428	349
10	105	393	335
50	105	352	316
100	105	337	311

temperature values of ε_r are relatively higher than reported compounds for same (ANb_2O_6) system [1,15]. The value of tan δ also increases with rise in temperature up to T_c and then decreases. The magnitude of tan δ also decreases on increasing frequencies. Variation of both ε_r and tan δ as a function of temperature (Fig. 3(a) and (b)) shows the occurrence of ferroelectric to para-electric transformation at phase transition, which is disturbed by a low temperature relaxation. The splitting between ferroelectric and relaxor behavior can only result from chemical ordering among cations occupying the same crystallographic site. In some cases, a ferroelectric phase can be electrically induced within the relaxor state [17,18].

The variation of real (Z') and imaginary (Z'') part or Nyquist plot of impedance with frequency at different temperatures is shown in Fig. 4. A single semicircular arc is appeared up to 75 °C. An intercept of semicircles on the real axis can give us bulk resistance of the material. From the trend of semicircles at different temperatures, it is indicated that the value of bulk resistance (R_b) decreases with rise in temperature up to 100 °C. At 100 °C, curve shows the two partially overlapping semicircles (shown in the inset (a) of Fig. 4) correspond to effective contribution of grains (the semicircle on the left-hand side) and grain boundaries (the semicircle on the right-hand side). Above 100 °C, second semicircular arc almost disappears (shown in the inset (b) of Fig. 4) or may be superimposed. Because of lack of experimental data in the higher frequency and temperature regions, we are unable to describe the resistive behavior of the compound. Above 100 °C, resistivity of the compound increases may be due to resulted in a super-imposition of the two elements (grain and grain boundary) as temperature increased [19].

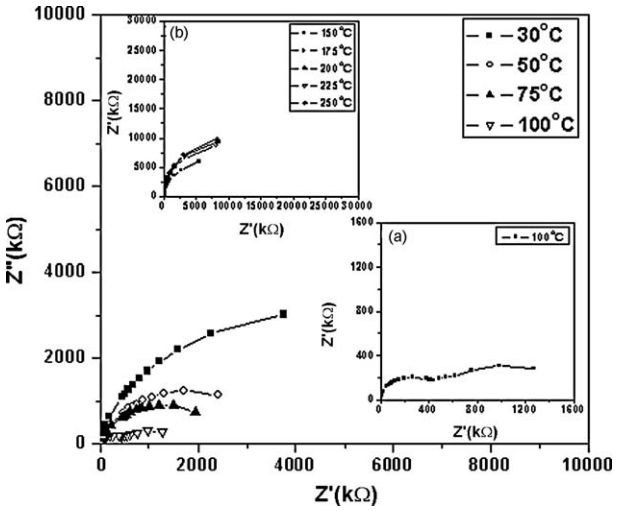

Fig. 4. Complex plane (Nyquist plot) representation of impedance in $SrNb_2O_6$.

The variation of real part of impedance (Z') as a function of frequency is shown in Fig. 5(a). Frequency dependence Z' shows a steep terrain in the low frequency region followed by a dispersive region. The plateau region becomes wider with rise in temperature extending up to 10 kHz. Above 10 kHz, the Z' variation appears to merge at all temperatures. The plateau region may be related to frequency invariant (dc) electrical property of the material and the final merger of the pattern at higher frequency may be attributed to the release of space charge. The value of Z' also shows a decreasing trend with rise in the temperature up to 100 °C, a phenomenon typical to the negative temperature coefficient of resistance (i.e., NTCR type behavior) as in semiconductors. Above 100 °C, compound shows some interesting (reverse) behavior, the magnitude of Z' increases with temperature increase that indicates a positive temperature coefficient of resistance (PTCR). Fig. 5(b) shows the loss spectrum (i.e., variation of imaginary impedance (Z'') with frequency) at various temperatures. The pattern of variation shows appearance of peaks at a characteristic frequency

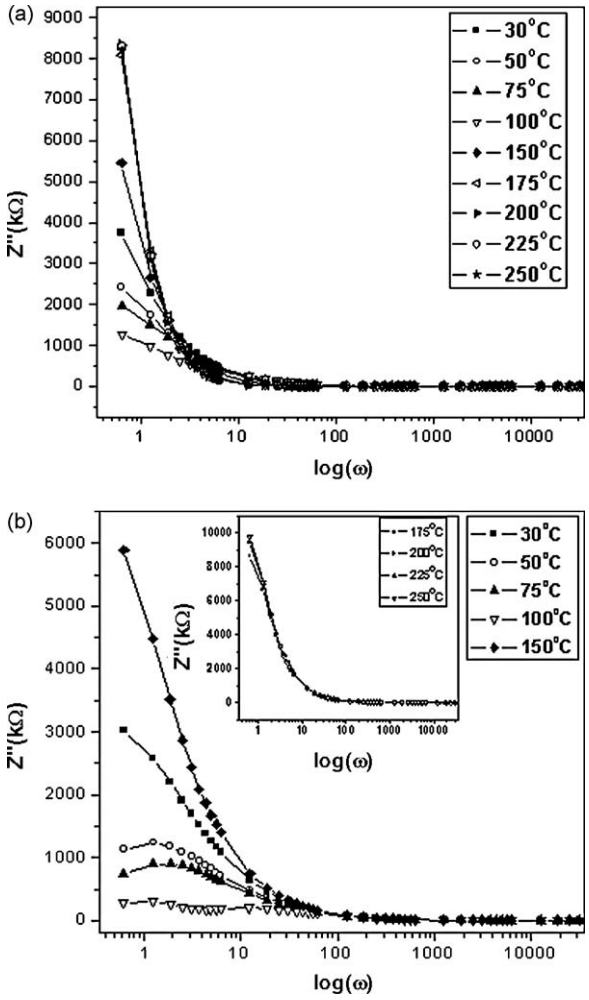

Fig. 5. (a) Plot of real part of impedance (Z') with frequency at different temperatures of $SrNb_2O_6$. (b) Plot of imaginary part of impedance (Z) with frequency at different temperatures of $SrNb_2O_6$.

dependent on temperature and can be related to the type and strength of the electrical relaxation phenomenon occurring in the material. A significant broadening of the peaks with rise in temperature suggests the presence of temperature dependent relaxation process in the material. The peak appears to be shifted towards higher frequency side with rise in temperature. The asymmetric broadening of the peaks may be attributed to the presence of electrical processes in the material with spread of relaxation time (indicated by peak width). Further, the magnitude of Z'' maxima decreases with rise in temperature up to 100 °C and then increases with rise in temperature (i.e., in between 100 and 175 °C). There are two peaks appeared at 100 °C, due to both grain and grain boundary contribution can be appeared at 100 °C. The contribution of grain boundaries is disappeared below 100 °C, may be because of lack of experimental data in the higher frequency. Above 175 °C, the value of Z'' is almost temperature independent and no peak appears over there, may be due to a superimposition of grain and grain boundary.

Fig. 6 exhibits the variation of real part of dielectric constant (ε') of $SrNb_2O_6$ with frequency at different temperatures. The values of ε' at low frequency are very high which decrease on increasing frequency. This is a normal behavior of dielectrics because at lower frequencies different types of polarizations (i.e., dipole, atomic, ionic, electronic, interfacial) are present in the compound. There is a step or gradual increase of ε' with increasing frequency. This qualitative behavior could be understood from Debye relation (represented by Eqs. (1) and (2), respectively) [20]:

$$\varepsilon'(\omega) = \frac{\varepsilon(s) - \varepsilon(\infty)}{1 + (\omega\tau)^2} \quad (1)$$

$$\varepsilon''(\omega) = \varepsilon(\infty) + \frac{\varepsilon(s) - \varepsilon(\infty)}{1 + (\omega\tau)^2} \quad (2)$$

where ω is the angular frequency ($\omega = 2\pi f$), $\varepsilon(s)$ and $\varepsilon(\infty)$ are the low and high frequency values of ε', respectively and τ is the relaxation time. Fig. 6(inset) shows the variation of ε'' with

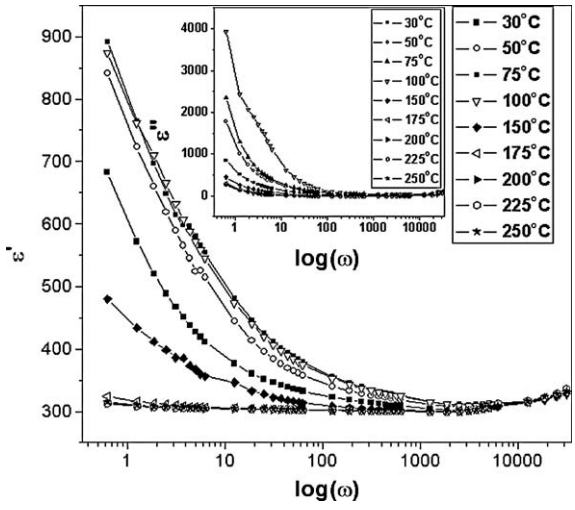

Fig. 6. The frequency dependence ε' in entire temperature range investigated. Inset shows the frequency dependence of ε'' at various temperature.

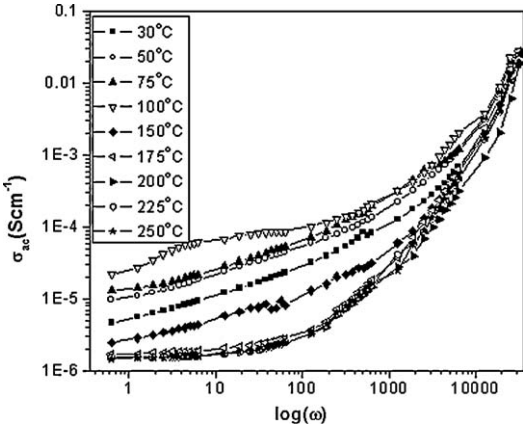

Fig. 7. Variation of ac conductivity as a function of frequency at different temperatures.

frequency at different temperatures. The peaks are not observed in the frequency plots of ε'' as shown in Fig. 6(inset). The value of ε'' decreases as the frequency increases. The value of ε' and ε'' first increases with increasing temperature and decreases further with increasing temperature. This also confirms that ferroelectric phase transition occurs in this range.

Fig. 7 shows the variation of ac conductivity (σ_{ac}) with frequency at different temperatures. The graph shows strong frequency dependence behavior of the compound at all temperatures. It is clearly observed in Fig. 7 that low and high frequency dispersive region can be separated by a change in slope at a certain value of frequency for each temperature. This frequency at which a change in the slope of conductivity spectrum occurs is conventionally known as the ''hopping frequency (ω_p)''. The values of hopping frequencies are observed to increase with the rise in temperature suggesting a possible enhancement in the carrier-hopping rate of the mobile charge carriers with rise in temperature. A conductivity behavior of this type is well described by Jonscher's universal power law equation [21]: $\sigma(\omega) = \sigma_{dc} + A\omega^n$, where n is the frequency exponent ($0 \leq n \leq 1$) and A is a pre-exponential factor dependent on temperature. At low frequencies, spectrum shows that the magnitude of ac conductivity rises with temperature (i.e., a thermally activated process) in good agreement with the observations from the impedance variation with frequency. But at high frequencies, the magnitudes of ac electrical conductivity are very close to each other, which is almost temperature independent.

4. Conclusion

Strontium niobate ($SrNb_2O_6$) was synthesized by using a standard solid-state reaction route. X-ray diffraction pattern of the compound confirms the formation of the orthorhombic (columbite) phase. The SEM micrograph indicated polycrystalline microstructure with different grain sizes and an almost homogeneous grain distribution over the surface of the sintered compound. The temperature variation of relative dielectric permittivity and tangent loss give evidence of the phase transition in studied temperature range.

Complex impedance analysis reveals both the bulk and grain boundary contribution, which are temperature dependent at lower frequency range and at higher frequency, behavior is almost temperature independent.

References

[1] H.J. Lee, K.S. Hong, S.J. Kim, I.T. Kim, Dielectric properties of MNb_2O_6 compounds (where M = Ca, Mn, Co, Ni, OR Zn), Mater. Res. Bull. 32 (1997) 847–855.

[2] R.C. Pullar, J.D. Breeze, N.McN. Alford, Characterization and microwave dielectric properties of $M^{2+}Nb_2O_6$ ceramics, J. Am. Ceram. Soc. 88 (2005) 2466–2471.

[3] Y.C. Zhang, Z.X. Yue, Z. Gui, L.T. Li, Microwave dielectric properties of $(Zn_{1-x}Mg_x)Nb_2O_6$ ceramics, Mater. Lett. 57 (2003) 4531–4534.

[4] A. Ananta, R. Brydson, N.W. Thomas, Synthesis, formation and characterization of $MgNb_2O_6$ powder in a columbite-like phase, J. Eur. Ceram. Soc. 19 (1999) 355–362.

[5] H. Brusset, H. Gillier-Pandraud, S.D. Voliotis, Etude du polymorphisme du metaniobate de strontium $SrNb_2O_6$, Mater. Res. Bull. 6 (1971) 5–14.

[6] S. Nomura, Ceramics for microwave dielectric resonator, Ferroelectrics 49 (1983) 61.

[7] S. Kawashima, M. Nishida, I. Ueda, H. Ouchi, Ba(Zn,Ta) O_3 ceramic with low dielectric loss, J. Am. Ceram. Soc. 66 (1983) 421–423.

[8] H. Tamura, T. Konoike, K. Wakino, Improved high-Q dielectric resonator with complex perovskite structure, J. Am. Ceram. Soc. 67 (1984), C–59–61.

[9] T. Kolodiazhnyi, A. Petric, A. Belous, O. V'yunov, O. Yanchevskij, Synthesis and dielectric properties of barium tantalates and niobates with complex perovskite structure, J. Mater. Res. 17 (2002) 3182–3189.

[10] C.L. Li, C.C. Chou, D.S. Tsai, Fabrication and electric properties of PZN-based ceramics using modified columbite method, J. Eur. Ceram. Soc. 25 (2005) 2197–2200.

[11] S.Y. Chen, C.M. Wang, S.Y. Cheng, The effect of pyrochlore phase on formation mechanism and electrical properties of perovskite PZMN relaxors, Mater. Chem. Phys. 49 (1997) 70–77.

[12] J. Kuwata, K. Uchino, S. Nomura, Diffuse phase transitions in lead zinc niobate, Ferroelectrics 22 (1979) 863–867.

[13] S.L. Swartz, T.R. Shrout, Fabrication of perovskite lead magnesium niobate, Mater. Res. Bull. 17 (1982) 1245–1250.

[14] G.A. Smolenskii, A.I. Agranovskaya, Dielectric polarization of a number of complex compounds, Sov. Phys. Solid State 1 (1959) 1429–1437.

[15] A. Belous, O. Ovchar, B. Jancar, J. Bezjak, The effect of non-stoichiometry on the microstructure and microwave dielectric properties of the columbites $A^{2+}Nb_2O_6$, J. Eur. Ceram. Soc. 27 (2007) 2933–2936.

[16] E. Wu, POWD, An Interactive Powder Diffraction Data Interpretation and Indexing Program, Ver. 2.1, School of Physical Sciences, Flinders University South Bedford Park, SA 5042 Australia.

[17] R. Sommer, N.K. Yushin, J.J. Van Der Klink, Polar metastability and an electric-field-induced phase transition in the disordered perovskite $Pb(Mg_{1/3}Nb_{2/3})O_3$, Phys. Rev. B 48 (1993) 13230–13237.

[18] E.V. Colla, E.Yu. Koroleva, A.A. Nabereznov, N.M. Okuneva, Lead magnoniobate behavior in applied electric field, Ferroelectrics 151 (1994) 337–342.

[19] S.-B. Lee, S.-H. Yoon, H. Kim, Positive temperature coefficient of resistivity in $Pb(Fe_{1/2}Nb_{1/2})O_3$ ceramics, J. Eur. Ceram. Soc. 24 (2004) 2465–2470.

[20] S. saha, T.P. Sinha, Low-temperature scaling behavior of $BaFe_{0.5}Nb_{0.5}O_3$, Phys. Rev. B 65 (2002), 134103(1–7).

[21] A.K. Jonscher, The 'universal' dielectric response, Nature 276 (1977) 673–679.